Journal of Mechanics in Medicine and Biology
Vol. 13, No. 3 (2013) 1350022 (13 pages)

DOI: 10.1142/S021951941350022X

World Scientific
www.worldscientific.com

PREDICTION OF MUSCLE FORCES USING STATIC OPTIMIZATION FOR DIFFERENT CONTRACTILE CONDITIONS

YUNUS ZIYA ARSLAN*

Department of Mechanical Engineering, Faculty of Engineering
Istanbul University, Avcilar, Istanbul 34320, Turkey
yzarslan@istanbul.edu.tr

AZIM JINHA

Human Performance Laboratory, University of Calgary
2500 University Drive N.W., Calgary, AB T2N 1N4, Canada
azim@kin.ucalgary.ca

MOTOSHI KAYA

Department of Physics, Graduate School of Science
University of Tokyo, 7-3-1 Hongo Bunkyo-ku, 113-0033 Tokyo, Japan
kaya@nanobio.phys.s.u-tokyo.ac.jp

WALTER HERZOG

Human Performance Laboratory, University of Calgary
2500 University Drive N.W., Calgary, AB T2N 1N4, Canada
wherzog@ucalgary.ca

Received 18 July 2012
Accepted 3 September 2012
Published 26 October 2012

In this study, we introduced a novel cost function for the prediction of individual muscle forces for a one degree-of-freedom musculoskeletal system. Unlike previous models, the new approach incorporates the instantaneous contractile conditions represented by the force-length and force-velocity relationships and accounts for physiological properties such as fiber type distribution and physiological cross-sectional area (PCSA) in the cost function. Using this cost function, it is possible to predict experimentally observed features of force-sharing among synergistic muscles that cannot be predicted using the classical approaches. Specifically, the new approach allows for predictions of force-sharing loops of agonistic muscles in one degree-of-freedom systems and for simultaneous increases in force in one muscle and decreases in a corresponding agonist. We concluded that the incorporation of the contractile conditions in the

*Corresponding author.

weighting of cost functions provides a natural way to incorporate observed force-sharing features in synergistic muscles that have eluded satisfactory description.

Keywords: Muscle force prediction; static optimization; contractile conditions.

1. Introduction

The accurate prediction of individual muscle forces during human movement is a prime area of research in biomechanics (for reviews, see Refs. 1–4). Theoretical calculation of individual muscle forces depends on solving the redundancy problem, which arises because the number of muscles crossing a joint typically exceeds the number of rotational degrees-of-freedom.[1] One common approach to this problem is to formulate a static optimization strategy.[5–13] In static optimization, a cost function is optimized independently for each time point of interest.[14] Typical cost functions take the form of a weighted sum of muscle forces raised to some non-linear power (>1.0). Often, this weighting is done using the physiological cross-sectional area (PCSA), the fiber type distribution, or the maximal isometric force of the synergistic target muscles.[15] However during movement, the contractile conditions of muscles change continuously, thereby altering the ability of muscles to contribute to movements, which becomes particularly important when predicting muscles forces across a wide range of movement conditions.

The purposes of this study were (1) to design a cost function for the prediction of individual muscle forces that is sensitive to changes in contractile conditions of muscles and (2) to compare the corresponding force predictions with experimentally measured muscle forces across a variety of tasks.

2. Methods

2.1. *Experimental procedure*

The experimentally determined individual muscle forces used for comparison with theoretical muscle force predictions were obtained from the cat hind limb for a wide range of locomotor conditions. The detailed explanation of the experimental protocol can be found in Ref. 16. A brief summary is given below.

Five cats were trained to walk on a walkway set at different slopes (30°, 45°, and 60° up-slope) and to walk and run on a motor-driven treadmill at different speeds (0.8–1.2 m/s). All procedures were approved by the Life Sciences Animal Ethics Committee of the University of Calgary.

2.1.1. *Muscle force measurements*

In order to measure the forces produced by soleus (SOL) and medial gastrocnemius (MG) muscles during the locomotion tasks, "E"-shaped, stainless steel tendon force transducers, which were surgically implanted onto the separated tendons of the SOL and MG, were used.[17] Measurements were conducted one week following surgery, which allowed for complete recovery.[18]

2.1.2. *Joint angle measurements*

In order to obtain knee, ankle, and metatarsophalangeal (MP) joint angles, five reflective markers were placed over the hip, knee, ankle, MP joint, and toe of the instrumented hind limb. Three-dimensional positions of these markers were recorded using a motion analysis system (60 Hz; VP310, Motion Analysis Cooperation, Santa Rosa, CA, USA). Ground reaction forces of the instrumented hind limb were recorded using two force platforms located in the center of the walkway (DRMC36, AMTI, Newton, MA, USA). Ground reaction forces were stored simultaneously with the muscle forces.

2.2. *Muscle length and muscle velocity analysis*

In this study, only the stance phase of the step cycle was analyzed since SOL and MG are not active during swing.[17] The stance phase was identified using the ground reaction forces, when available, or the high-speed video images. Muscle–tendon lengths of MG and SOL were calculated using the joint kinematics and the tendon travel technique.[19] Changes in muscle lengths were calculated as the first time derivative of muscle–tendon length using a quintic spline function.[20]

2.3. *Model of the musculoskeletal system*

A two-dimensional musculoskeletal model with one rotational degree-of-freedom for the cat ankle (flexion/extension) was developed (Fig. 1). The lines of action of SOL and MG muscles were modeled as straight lines crossing the ankle joint. In the model, f_1, f_2, and h denote the muscle forces of SOL and MG and the ankle joint moment, respectively. It was assumed that the moment arms of SOL and MG about the ankle were constant for walking and trotting.[21]

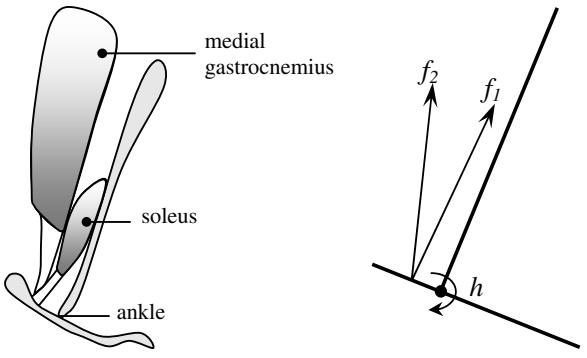

Fig. 1. (a) Anatomical and (b) musculoskeletal model of the cat foot, shank, and ankle.

2.4. *Optimal design problem*

The static optimization problem for solving for individual muscle forces was formulated as follows:

$$\text{Minimize } \{\phi(\boldsymbol{f})\}, \quad \phi(\boldsymbol{f}) = \sum_{i}^{n} \frac{(f_i v_i)^2 + \omega (f_i l_i)^2}{F_i(v_i) F_i(l_i) S_i} \tag{1}$$

subject to

$$h - \sum_{i=1}^{n} \boldsymbol{d}\boldsymbol{f}^T = 0, \quad f_i \geq 0, \quad i = 1, 2. \tag{2}$$

Here, $\phi(\boldsymbol{f})$, f_i, $F_i(v_i)$, $F_i(l_i)$, and S_i denote the objective function, unknown muscle forces, maximal muscle forces at instantaneous muscle contraction velocity v_i, maximal muscle force at instantaneous muscle length l_i, and the percentage of slow-twitch muscle fibers, respectively. ω was assumed constant and equal to 1 (in unit of $1/\text{s}^2$). In the constraint Eq. (2), $\boldsymbol{d}$ represents the moment arm vector at the ankle. The resultant ankle moment h was calculated using experimentally measured muscle forces.

The maximal muscle force at an instantaneous muscle contraction velocity $F_i(v_i)$ is given by the following equations[22]:

$$F_i(v_i) = \begin{cases} 0, & v_{0i} < v_i \\ \dfrac{F_{0i} b_i - a_i v_i}{v_i + b_i}, & 0 < v_i \leq v_{0i} \\ 1.5F_{0i} - 0.5 \dfrac{F_{0i} \frac{b_i}{2} + a_i v_i}{-v_i + \frac{b_i}{2}}, & -\dfrac{v_{0i}}{2} < v_i \leq 0 \\ 1.5F_{0i}, & v_i \leq -\dfrac{v_{0i}}{2} \end{cases} \tag{3}$$

Here, F_{0i} is the maximal isometric force a muscle can exert, v_{0i} is the maximal shortening velocity at which point force is zero, and a_i and b_i are Hill's thermodynamic constants for the ith muscle which were chosen as $0.25/F_{0i}$ and $0.25/v_{0i}$, respectively.[22,23]

The maximal muscle force at an instantaneous muscle length $F_i(l_i)$ was calculated as:

$$F_i(l_i) = F_{iac}(l_i) + F_{ipas}(l_i). \tag{4}$$

The maximal active muscle force $F_{iac}(l_i)$, was calculated from the relationship between force and length at the muscle level. The passive muscle force $F_{ipas}(l_i)$ was obtained from[24]:

$$F_{ipas}(l_i) = 1.3F_{0i} \arctan\left(0.1\left(\frac{l_i}{l_0} - 0.22\right)^{10}\right), \tag{5}$$

where l_0 denotes the optimal muscle length at which active force is maximal. All the muscle parameters used in the study are given in Appendix (Table A.1).

Minimizing the proposed objective function favors muscles with favorable contractile conditions and punishes muscles with poor contractile conditions. Contractile conditions of muscles have a profound effect on force-sharing among synergistic muscles, which becomes particularly apparent when some muscles in a synergistic group are driven to their contractile limits.[25,26] By incorporating $F_i(v_i)$ and $F_i(l_i)$ as weighting factors into the cost function, the force−velocity and force−length properties of the synergistic muscles become crucial determinants in the determination of the unknown muscle forces.[27] $F_i(v_i)$ and $F_i(l_i)$ partly depend on the PCSA; thus, PCSA was included in the cost function in an indirect manner. The percentage of slow-twitch muscle fiber S_i, which reflects muscle endurance, was incorporated into Eq. (1) as a weighting factor.[6]

The proposed cost function was solved analytically using the Karush−Kuhn−Tucker theorem.[28] Applying this theorem to Eq. (1) gives the following:

$$f_i = \frac{d_i}{d_j}\frac{F_i(v_i)}{F_j(v_j)}\frac{F_i(l_i)}{F_j(l_j)}\frac{S_i}{S_j}\left(\frac{v_j^2 + l_j^2}{v_i^2 + l_i^2}\right) f_j. \tag{6}$$

The unknown muscle forces f_i, f_j can be determined by solving Eq. (6) with the moment equilibrium condition (Eq. (2)).

Prilutsky *et al.*[29] compared theoretically obtained muscle forces, which were calculated by six different cost functions with experimentally measured cat muscle forces, and they showed that the cost function proposed by Dul *et al.*[6] predicted unknown muscle forces better than the others. Schappacher-Tilp *et al.*[27] improved the cost function by Dul *et al.*[6] by replacing maximal isometric force with the maximal force as a function of the speed of shortening as the weighting factor. The cost function proposed by Schappacher-Tilp *et al.*[27] is given by

$$\begin{aligned} &\text{Minimize } \left\{\max\left(\frac{1}{q_i}\left(100\,\frac{f_i}{F_i(v_i)}\right)^{-p_i}\right)\right\} \\ &\text{subject to Eq. (2),} \end{aligned} \tag{7}$$

where p_i and q_i are functions of the percentage of slow-twitch fibers and are defined by Dul *et al.*[6] Hereafter, the cost function proposed in this study will be referred to as Cost Function I and the cost function proposed by Schappacher-Tilp *et al.*[27] as Cost Function II. In order to evaluate Cost Function I, force predictions of Cost Function I were compared to those of Cost Function II.

2.5. *Error analysis*

The number of step cycles used for error analysis ($n = 5$ cats), and the different walking and trotting conditions are given in Table 1. Null cells of Table 1 denote conditions that a cat did not perform. A total of 188 step cycles were used to analyze the force predictions of Cost Functions I and II.

Table 1. Number of step cycles.

Condition	Cat 1	Cat 2	Cat 3	Cat 4	Cat 5
60° upslope	14	5	4	4	—
45° upslope	11	4	9	29	13
30° upslope	17	7	8	11	15
level	9	—	—	—	28
Total step cycle	51	16	21	44	56

In order to evaluate the individual muscle force prediction quantitatively, root mean square differences (RMSD) and Pearson correlation coefficients (PCC) were calculated between the experimentally measured and the theoretically predicted force-time histories.[30,31] In our case, RMSD and PCC measure the similarity in magnitude and shape between predicted and actual force-time histories, respectively. A RMSD value of 0.01 means that the predicted forces have a 1% mean error from the measured forces. A PCC value of 0 indicates that the predicted and measured forces are uncorrelated, while a PCC value of 1.0 indicates that the predicted and measured forces are perfectly correlated. Furthermore, ANOVA was used to analyze statistically significant differences in average RMSD (e) and average PCC (r) obtained from Cost Functions I and II. The level of significance was set at $p = 0.05$ for all statistical testing.

3. Results

Comparison of the typical patterns of muscle forces obtained using Cost Functions I and II with the experimentally measured forces are depicted for 45° upslope and level walking in Fig. 2. Moreover, typical patterns of predicted and measured force-sharing loops for SOL and MG are shown in Fig. 3. Arrows indicate the direction of loop formation.

For a quantitative error analysis, RMSD and PCC values between predicted and measured force-time histories were calculated for each step cycle and the corresponding averages of RMDS and PCC values (e and r, respectively) for each case (16 different cases) are presented in Table 2. Final average values of e and r, along with the results of the statistical analysis, are presented in Fig. 4.

Values for e obtained from Cost Function I ranged between 0.31 and 0.82 for SOL, and between 0.03 and 0.79 for MG (Table 2). Values for r obtained from Cost Function I ranged between 0.515 and 0.884 for SOL and between 0.940 and 0.998 for MG. For Cost Function II, e values ranged between 0.575 and 1.847 for SOL, and between 0.06 and 0.56 for MG. Values for r obtained using Cost Function II ranged between 0.246 and 0.870 for SOL and between 0.948 and 0.993 for MG.

Cost Function I showed better SOL force predictions than Cost Function II in 12 of the 16 cases according to the e values and in 14 of the 16 cases according to the r values (Table 2). Cost Function I performed statistically significantly better than

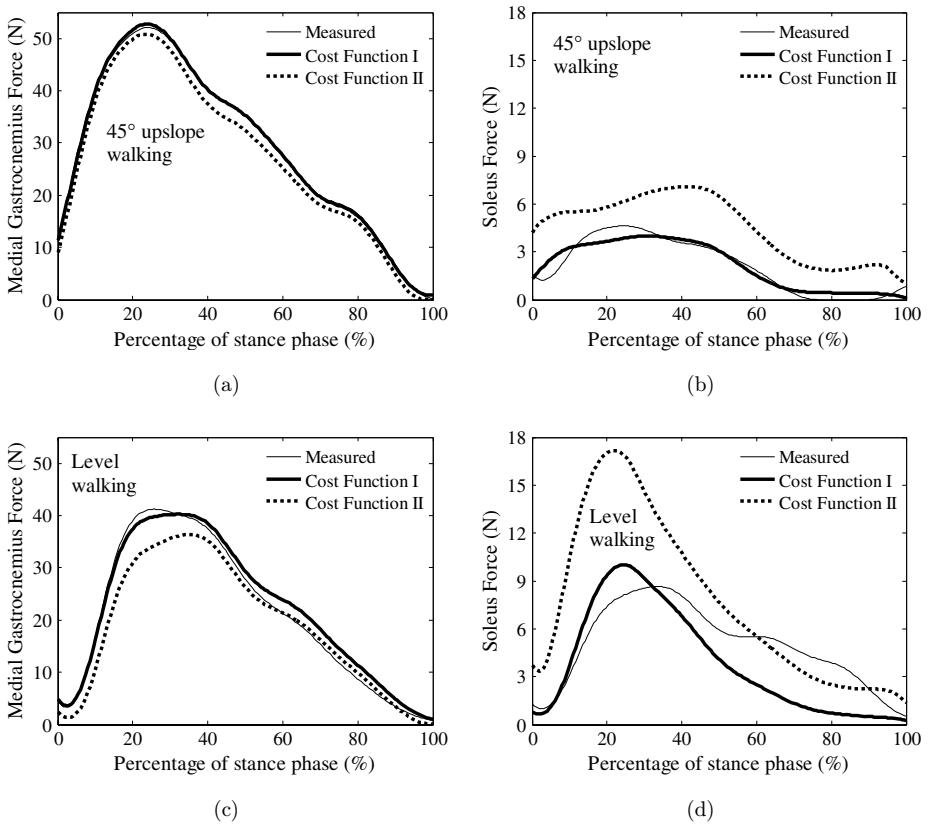

Fig. 2. Comparison of the experimentally measured SOL and MG forces with theoretically predicted forces obtained from Cost Function I and II for (a), (b) 45° up-slope walking on walkway and (c), (d) level walking on treadmill.

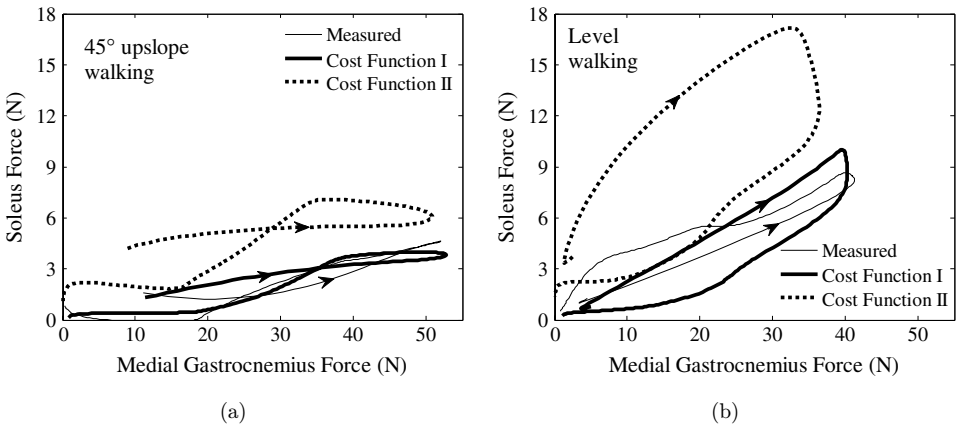

Fig. 3. Typical force-sharing patterns between SOL and MG muscles for (a) 45° up-slope walking on walkway and (b) level walking on treadmill.

Table 2. Calculated e and r values of SOL and MG.

	Cost Function I				Cost Function II			
	SOL		MG		SOL		MG	
Cases	$e \pm sd$	$r \pm sd$	$e \pm sd$	$r \pm sd$	$e \pm sd$	$r \pm sd$	$e \pm sd$	$r \pm sd$
Cat I								
60° upslope	0.80 ± 0.39	0.628 ± 0.170	0.04 ± 0.02	0.995 ± 0.005	1.26 ± 0.64	0.497 ± 0.310	0.07 ± 0.03	0.990 ± 0.012
45° upslope	0.77 ± 0.44	0.515 ± 0.309	0.05 ± 0.02	0.992 ± 0.006	1.15 ± 0.68	0.531 ± 0.365	0.08 ± 0.04	0.990 ± 0.011
30° upslope	0.75 ± 0.43	0.628 ± 0.186	0.06 ± 0.02	0.993 ± 0.005	1.48 ± 0.90	0.556 ± 0.254	0.13 ± 0.05	0.987 ± 0.010
level/fast	0.77 ± 0.26	0.695 ± 0.251	0.17 ± 0.09	0.993 ± 0.004	0.94 ± 0.41	0.246 ± 0.326	0.19 ± 0.08	0.986 ± 0.011
Cat II								
60° upslope	0.54 ± 0.12	0.602 ± 0.244	0.05 ± 0.01	0.988 ± 0.007	1.87 ± 0.09	0.359 ± 0.276	0.17 ± 0.01	0.948 ± 0.015
45° upslope	0.58 ± 0.07	0.678 ± 0.067	0.12 ± 0.01	0.989 ± 0.002	0.64 ± 0.08	0.601 ± 0.133	0.14 ± 0.01	0.973 ± 0.008
30° upslope	0.59 ± 0.08	0.690 ± 0.128	0.13 ± 0.03	0.990 ± 0.004	0.57 ± 0.18	0.632 ± 0.124	0.11 ± 0.02	0.974 ± 0.011
Cat III								
60° upslope	0.78 ± 0.02	0.749 ± 0.144	0.41 ± 0.10	0.976 ± 0.025	0.55 ± 0.06	0.695 ± 0.230	0.29 ± 0.03	0.975 ± 0.016
45° upslope	0.79 ± 0.03	0.707 ± 0.128	0.54 ± 0.06	0.959 ± 0.014	0.56 ± 0.02	0.650 ± 0.193	0.39 ± 0.04	0.953 ± 0.017
30° upslope	0.82 ± 0.04	0.700 ± 0.121	0.79 ± 0.31	0.940 ± 0.040	0.59 ± 0.03	0.655 ± 0.149	0.56 ± 0.20	0.923 ± 0.051
Cat IV								
60° upslope	0.55 ± 0.24	0.780 ± 0.074	0.04 ± 0.02	0.996 ± 0.002	1.39 ± 0.52	0.712 ± 0.215	0.10 ± 0.03	0.992 ± 0.007
45° upslope	0.42 ± 0.20	0.785 ± 0.165	0.03 ± 0.01	0.996 ± 0.005	0.77 ± 0.39	0.764 ± 0.181	0.06 ± 0.03	0.993 ± 0.012
30° upslope	0.58 ± 0.16	0.741 ± 0.108	0.05 ± 0.01	0.993 ± 0.002	1.45 ± 0.38	0.667 ± 0.142	0.14 ± 0.03	0.980 ± 0.009
Cat V								
45° upslope	0.31 ± 0.09	0.884 ± 0.051	0.03 ± 0.00	0.998 ± 0.000	1.15 ± 0.21	0.780 ± 0.061	0.12 ± 0.01	0.992 ± 0.002
30° upslope	0.39 ± 0.05	0.863 ± 0.039	0.08 ± 0.02	0.996 ± 0.001	0.63 ± 0.11	0.870 ± 0.038	0.13 ± 0.02	0.993 ± 0.003
level/fast	0.48 ± 0.08	0.813 ± 0.066	0.08 ± 0.04	0.994 ± 0.003	0.74 ± 0.23	0.698 ± 0.115	0.12 ± 0.02	0.985 ± 0.007

Note: e: average root mean square difference; sd: standard deviation; r: average Pearson correlation coefficient.

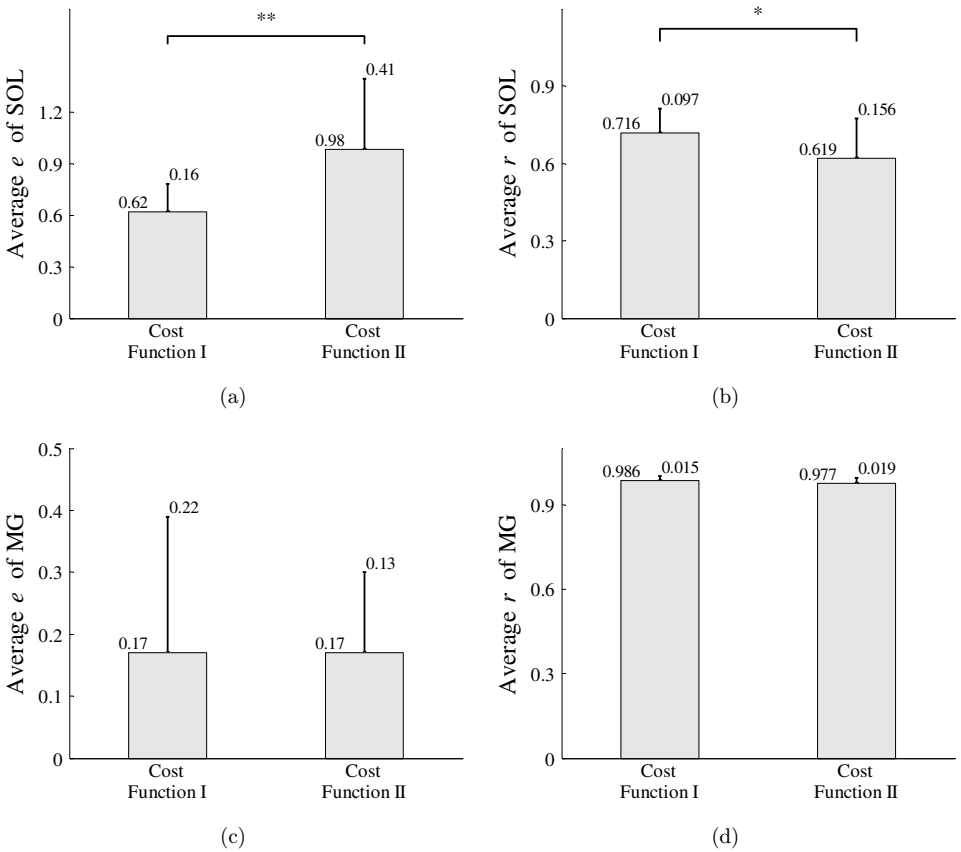

Fig. 4. Mean ($\pm sd$) values for e and r for 16 experimental conditions, $^*p < 0.05$, $^{**}p < 0.01$.

Cost Function II for SOL (Figs. 4(a) and 4(b)). MG force predictions with Cost Function I gave smaller e values than those obtained with Cost Function II in 12 of the 16 cases (Table 2). In addition, Cost Function I gave better predictions (r) of force−time histories in all of the 16 cases than Cost Function II. Moreover, forces predicted using Cost Function I had equal average e values to and higher average r values than forces predicted using Cost Function II (Figs. 4(c) and 4(d)).

4. Discussion

Individual muscle force measurements in the cat hind limb have shown that force-sharing between synergistic muscles is highly task-dependent and cannot be captured with a constant weighting factor in the cost function.[16,17] For example, peak SOL forces are consistently greater than peak MG forces during slow and medium speeds (0.4−0.8 m/s) level walking,[29] while peak MG forces become much greater than SOL forces for running, jumping, and up-slope walking. During quiet standing, cat SOL

muscles produce up to 50% of their maximum isometric forces, while MG is completely silent.[25] The exact opposite occurs during scratching or paw-shaking where MG is highly activated and produces substantial forces, while SOL is often not activated and its contribution is purely passive.[32–34] One of the explanations for this dramatic difference in task-dependent force production between SOL and MG is the difference in the composition of fibre types — 98% slow-twitch for SOL and about 37% slow-twitch for MG,[35–37] and the associated differences in force-length and force-velocity properties.[21,38] Therefore, force predictions for these muscles using static optimization have been bad, as traditional cost functions with constant weighting factors[1,6,8,15,18,29,39] cannot predict some of the most basic observations, for example a loop-type force-sharing behavior between synergistic muscles in a one degree-of-freedom model, or the increase in force in one agonist with a simultaneous decrease in force in another agonist.

Schappacher-Tilp *et al.*[27] introduced a conceptually new set of cost functions that overcame the problems of previous static optimization approaches by formulating a cost function with a variable weighting factor, based on the force-velocity relationship, but neglecting other mechanical properties such as the force-length relationship. Also, Schappacher-Tilp *et al.*[27] demonstrated the increased flexibility of these types of cost functions, but there was no attempt at comparing the results to actual muscle forces measured during unrestrained movements.

Here, we demonstrated that the proposed cost function that includes the instantaneous contractile conditions of the target muscles, along with the physiological properties of muscular contraction, gives satisfactory results in predicting cat SOL and MG force-time histories and their associated force-sharing loops. Since traditional cost functions cannot predict loop-type force-sharing behavior for the system studied here, and cannot predict decreasing SOL forces with increasing MG forces[27] as observed experimentally in this study, it is obvious, and has been argued previously, that classical cost functions of the type introduced first by Crowninshield and Brand[1,15] and used more than any other cost functions[6,8,12,39–42] cannot be used to make accurate force predictions for individual muscles during unrestrained movements. Therefore, we suggest that accurate individual muscle force predictions are possible when accounting for the instantaneous contractile conditions and knowing their force-length and force-velocity properties.

Needless to say that we realize that such properties remain unknown for most human muscles and measuring the instantaneous contractile conditions of skeletal muscles has been impossible, except for constrained movements in laboratory settings[43–45] and for isolated muscles only.[46,47] Therefore, although the proposed cost function can probably be used to formulate more accurate predictions of individual muscle forces than the traditionally used cost functions, it cannot compete with the simplicity of the traditional cost functions, which do not require contractile information about the target muscles,[48] but rely on minimal information such as the muscles' PCSA[1,15] or the percentage of slow-twitch fibers.[6] The simplicity of the traditional cost functions has likely been the major factor contributing to their extensive use.

5. Conclusion

The cost function proposed here accounts for the instantaneous contractile conditions and incorporates the basic mechanical properties of muscles. For this reason, it can predict experimentally observed force-sharing behavior, such as force-sharing loops and simultaneous increase in force in one agonist and decrease in another, which cannot be predicted with traditional cost functions. However, the cost function proposed here requires information for implementation and evaluation that can presently only be obtained using invasive approaches in animal models of force-sharing and thus, will likely not be readily available in the near future for human force predictions.

Acknowledgement

This work was supported by the Scientific and Technological Research Council of Turkey (TUBITAK).

References

1. Crowninshield RD, Brand RA, The prediction of forces in joint structures: Distribution of intersegmental resultants, *Exerc Spotr Sci Rev* **9**:159−181, 1981.
2. Herzog W, Force-sharing among synergistic muscles: Theoretical considerations and experimental approaches, *Exerc Spotr Sci Rev* **24**:173−202, 1996.
3. Tsirakos D, Baltzopoulos V, Bartlett R, Inverse optimization: Functional and physiological considerations related to the force-sharing problem, *Crit Rev Biomed Eng* **25**(4−5):371−407, 1997.
4. Erdemir A, McLean S, Herzog W, van den Bogert AJ, Model-based estimation of muscle forces exerted during movements, *Clin Biomech* **22**(2):131−154, 2007.
5. Penrod DD, Davy DT, Singh DP, An optimization approach to tendon force analysis, *J Biomech* **7**(2):23−129, 1974.
6. Dul J, Johnson GE, Shiavi R, Townsend MA, Muscular synergism-II. A minimum-fatigue criterion for load sharing between synergistic muscles, *J Biomech* **17**(9):675−684, 1984.
7. Bean JC, Chaffin DB, Schultz AB, Biomechanical model calculation of muscle contraction forces: A double linear programming method, *J Biomech* **21**(1):59−66, 1988.
8. Kaufman KR, An K-N, Litchy WJ, Chao EYS, Physiological prediction of muscle forces-I. Theoretical formulation, *Neuroscience* **40**(3):781−792, 1991.
9. Van der Helm FCT, A finite element musculoskeletal model of the shoulder mechanism, *J Biomech* **27**(5):551−569, 1994.
10. Raikova R, Aladjov H, The influence of the way the muscle force is modeled on the predicted results obtained by solving indeterminate problems for a fast elbow flexion, *Comput Methods Biomech Biomed Eng* **6**(3):181−196, 2003.
11. Czaplicki A, Silva M, Ambrósio J, Jesus O, Abrantes J, Estimation of the muscle force distribution in ballistic motion based on a multibody methodology, *Comput Methods Biomech Biomed Eng* **9**(1):45−54, 2006.
12. Praagman M, Chadwick EKJ, van Der Helm FCT, Veeger HEJ, The relationship between two different mechanical cost functions and muscle oxygen consumption, *J Biomech* **39**(4):758−765, 2006.

13. Heintz S, Gutierrez-Farewik E, Static optimization of muscle forces during gait in comparison to EMG-to-force processing approach, *Gait Posture* **26**(2):279−288, 2007.
14. Hardt DE, Determining muscle forces in the leg during normal human walking — an application and evaluation of optimization methods, *J Biomech Eng* **100**:72−78, 1978.
15. Crowninshield RD, Brand RA, A physiologically based criterion of muscle force prediction in locomotion, *J Biomech* **14**(1):793−801, 1981.
16. Kaya M, Leonard T, Herzog, W, Coordination of medial gastrocnemius and soleus forces during cat locomotion, *J Exp Biol* **206**:3645−3655, 2003.
17. Herzog W, Leonard TR, Guimaraes CS, Forces in gastrocnemius, soleus, and plantaris tendons of the freely moving cat, *J Biomech* **26**(8):945−953, 1993.
18. Herzog W, Leonard TR, Validation of optimization models that estimate the forces exerted by synergistic muscles, *J Biomech* **24**(Suppl 1):31−39, 1991.
19. Muraoka T, Muramatsu T, Fukunaga T, Kanehisa H, Influence of tendon slack on electromechanical delay in the human medical gastrocnemius *in vivo*, *J Appl Physiol* **36**(2):540−544, 2004.
20. Woltring HJ, A fortran package for generalized, cross-validatory spline smoothing and differentiation, *Adv Eng Softw* **8**:104−113, 1986.
21. Herzog W, Leonard TR, Renaud JM, Wallace J, Chaki G, Bornemisza S, Force-length properties and functional demands of cat gastrocnemius, soleus and plantaris muscles, *J Biomech* **25**(11):1329−1335, 1992
22. Epstein M, Herzog W, *Theoretical Models of Skeletal Muscle: Biological and Mathematical Considerations*, John Wiley & Sons, New York, 1998.
23. Hill AV, The heat of shortening and the dynamic constants of muscle, *Proc R Soc Lond B* **126**:136−195, 1938.
24. Pennestri E, Stefanelli R, Valentini PP, Vita L, Virtual musculo-skeletal model for the biomechanical analysis of the upper limb, *J Biomech* **40**(6):1350−1361.
25. Hodgson JA, The relationship between soleus and gastrocnemius muscle activity in conscious cats — a model for motor unit recruitment? *J Physiol* **337**:553−562, 1983.
26. Kaya M, Leonard TR, Herzog W, Premature deactivation of soleus during the propulsive phase of cat jumping, *J R Soc Interface* **5**(21):415−426, 2008.
27. Schappacher-Tilp G, Binding P, Braverman E, Herzog W, Velocity-dependent cost function for the prediction of force sharing among synergistic muscles in a one degree of freedom model, *J Biomech* **42**(5):657−660, 2009.
28. Bazaraa MS, Sherali HD, Shetty CM, *Nonlinear Programming Theory and Algorithms*, John Wiley & Sons, New York, 1993.
29. Prilutsky BI, Herzog W, Allinger TL, Forces of individual cat ankle extensor muscles during locomotion predicted using static optimization, *J Biomech* **30**(10):1025−1033, 1997.
30. Savelberg HHCM, Herzog W, Prediction of dynamic tendon forces from electromyographic signals: An artificial neural network approach, *J Neurosci Methods* **78**(1−2):65−74, 1997.
31. Luh JJ, Chang GC, Cheng CK, Lai JS, Kuo TS, Isokinetic elbow joint torques estimation from surface EMG and joint kinematic data: Using an artificial neural network model, *J Electromyogr Kines* **9**(3):173−183, 1999.
32. Smith JL, Betts B, Edgerton VR, Zernicke RF, Rapid ankle extension during paw shakes — selective recruitment of fast ankle extensors, *J Neurophysiol* **43**(3):612−620, 1980.
33. Abraham LD, Loeb GE, The distal hindlimb musculature of the cat. Patterns of normal use, *Exp Brain Res* **58**(3):580−593, 1985.
34. Herzog W, Force sharing among the primary cat ankle muscles, *Eur J Morphol* **36**:280−287, 1998.

35. Ariano MA, Armstrong RB, Edgerton VR, Hindlimb muscle fiber populations of five mammals, *J Histochem Cytochem* **21**(1):51−55, 1973.
36. Burke RE, Levine DN, Tsairis P, Zajac FE, Physiological types and histochemical profiles in motor units of the cat gastrocnemius, *J Physiol* **234**(3):723−748, 1973.
37. Burke RE, Levine DN, Salcman M, Tsairis P, Motor units in cat soleus muscle: Physiological, histochemical and morphological characteristics, *J Physiol* **238**(3):503−514.2, 1974.
38. Spector SA, Gardiner PF, Zernicke RF, Roy RR, Edgerton VR, Muscle architecture and force-velocity characteristics of cat soleus and medial gastrocnemius: Implications for motor control, *J Neurophysiol* **44**(5):951−960, 1980.
39. Raikova R, A model of the flexion-extension motion in the elbow joint some problems concerning muscle forces modelling and computation, *J Biomech* **29**(6):763−772, 1996.
40. Patriarco AG, Mann RW, Simon, SR, Mansour, JM, An evaluation of the approaches of optimization models in the prediction of muscle forces during human gait, *J Biomech* **14**(8):513−525, 1981.
41. Happee R, van Der Helm FCT, The control of shoulder muscles during goal directed movements, an inverse dynamic analysis, *J Biomech* **28**(10):1179−1191, 1995.
42. Li G, Kaufman KR, Chao EY, Rubash HE, Prediction of antagonistic muscle forces using inverse dynamic optimization during flexion/extension of the knee, *J Biomech Eng* **121**(3):316−322, 1999.
43. Fukunaga T, Ichinose Y, Ito M, Kawakami Y, Fukashiro S, Determination of fascicle length and pennation in a contracting human muscle *in vivo*, *J Appl Physiol* **82**(1):354−358, 1997.
44. Ichinose Y, Kawakami Y, Ito M, Kanehisa H, Fukunaga T, *In vivo* estimation of contraction velocity of human vastus lateralis muscle during "isokinetic" action, *J Appl Physiol* **88**(3):851−856, 2000.
45. Kaya M, Coordination of cat hindlimb muscles during voluntary movements, Ph.D. Thesis, University of Calgary, 2003.
46. Scott SH, Brown IE, Loeb GE, Mechanics of feline soleus: I. Effect of fascicle length and velocity on force output, *J Muscle Res Cell Motil* **17**(2):207−219, 1996.
47. Kaya M, Carvalho W, Leonard T, Herzog W, Estimation of cat medial gastrocnemius fascicle lengths during dynamic contractions, *J of Biomech* **35**(7):893−902, 2002.
48. Pedotti A, Krishnan VV, Stark L, Optimization of muscle-force sequencing in human locomotion, *Math Biosci* **38**(1−2):57−76, 1978.

Appendix

Table A.1. Muscle parameters used in the study.

Parameters	SOL	MG
d (m)	0.016	0.019
$PCSA$ (cm^2)	0.91	4.01
F_0 (N)	20.8	96.5
v_0 (m/s)	0.176	0.258
l_0 (m)	0.102	0.120
S (%)	98	37